Wärme- und Stoffübertragung 8 (1975) 193-202


# Combined Influence of Hall Effect, Ion Slip, Viscous Dissipation and Joule Heating on MHD Heat Transfer in a Channel

V. Javeri, Berlin

Abstract. To investigate the combined influence of Hall effect, ion slip, viscous dissipation and Joule heating on the fully developed laminar MHD channel heat transfer, the exact solution of the energy equation is derived assuming a constant wall heat flux, finely segmented electrodes and a small magnetic Reynolds number. It is concluded that there can be a substantial difference, depending upon Hartmann number, electric field intensity and Brinkman number, between the Nusselt number considering the Hall effect and that neglecting it. Representative results are presented in diagrams and in tables.

Zusammenfassung. Um den Gesamteinfluß des Hall-Effekts, Ionenschlupfes, der viskosen Dissipation and Jouleschen Erwärmung auf die laminare Wärmeübertragung in einem MHD-Kanal zu untersuchen, ist die exakte Lösung der Energiegleichung abgeleitet, wobei man konstante Wärmestromdichte an der Kanalwand, unendlich fein segmentierte Elektroden und kleine magnetische Reynolds-Zahl annimmt. Es ist festgestellt, daß abhängig von der Hartmann-Zahl, elektrischen Feldstärke und Brinkman-Zahl ein wesentlicher Unterschied zwischen der Nusselt-Zahl, die den Hall-Effekt berücksichtigt, und der, die ihn vernachlässigt, bestehen kann. Typische Ergebnisse sind in den Bildern und Tabellen dargestellt.

Nomenclature

| | |
|---|---|
| A | channel cross section |
| B | magnetic induction |
| Br | Brinkman number |
| E | electric field |
| Ec | Eckert number |
| Ha | Hartmann number |
| Nu | Nusselt number |
| Pe | Peclet number |
| Pr | Prandtl Number |
| Q | heat generation function, Eq. (12) |
| Re | Reynolds number |
| T | temperature |
| c | half channel height |
| $c_p$ | specific heat at constant pressure |
| f | mass fraction of unionized particles |
| h | specific enthalpy |
| j | current density |
| p | pressure |
| q | heat flux |
| t | time |
| v | velocity |
| x, y, z | cartesian coordinate |
| $\beta_e$ | Hall parameter |
| $\beta_I$ | ion slip parameter |
| $\delta_{ij}$ | Dirac delta function |
| $\eta$ | dynamic viscosity |
| $\lambda$ | thermal conductivity |
| $\mu$ | magnetic permeability |
| $\nu$ | kinematic viscosity |
| $\rho$ | mass density |
| $\rho_e$ | charge density |
| $\sigma$ | electrical conductivity |
| $\tau$ | shear stress tensor |
| $\Phi$ | dissipation function |

Subscripts

| | |
|---|---|
| c | conduction |
| j | Joule heating, Eq. (14) |
| m | mean value |
| mag | magnetic |
| q | heat flux, Eq. (14) |
| ref | reference value |
| v | viscous dissipation, Eq. (14) |
| w | wall |
| x, y, z | cartesian coordinate direction |

Superscripts

| | |
|---|---|
| $\rightarrow$ | vector |
| + | substantial quantity, Eqs. (2) and (3) |
| ' | reduced quantity, Eqs. (9c) and (10) |
| - | dimensionless quantity, Eq. (10) |

## 1. Introduction

The asymptotic fully developed temperature distribution corresponding to the classical Hartmann velocity profile for the magnetohydrodynamic (MHD) channel flow was derived for the first time by Perlmutter and Siegel [1]. In their analysis, the internal heat generation due to viscous dissipation and Joule heating was included and the constant wall heat flux was assumed. Their analysis is valid only for the fluids, which have a non-tensor electrical conductivity throughout the channel.

In an MHD device using partially ionized gases, the approximation of a constant electrical conductivity of the working medium is not reasonable. In this case, one has to consider the influence of the tensor conductivity due to Hall effect and ion slip on the velocity field. For example, if solid electrodes are used in an MHD generator, then a Hall current will be produced in the flow direction with a subsequent reduction in the effective electrical conductivity and power density. Further, the usual viscous velocity profile in the flow direction will interact with Hall currents to cause transverse velocities.

Eraslan [2] solved the energy equation numerically, where he considered the combined effect of viscosity and tensor conductivity on velocity field in a flat channel, assumed the constant wall temperature and neglected the temperature gradient in the flow direction.

In a previous paper, Javeri [4] derived the velocity and temperature distributions in a closed form for an MHD channel flow, where the influence of viscosity, Hall effect and ion slip on the hydrodynamic fields was investigated. Javeri [4] assumed a constant wall heat flux and neglected the internal heat generation completely.

The purpose of this paper is to extend the analysis of Javeri [4] and to explore the combined influence of Hall effect, ion slip, viscous dissipation and Joule heating on the temperature field and heat transfer in a flat channel. Including this combined influence, the exact solution of the energy equation is derived for the boundary condition of second kind for temperature.

## 2. Analysis

### 2.1. Generalized Equations

For the physical model, which is formulated by Sutton and Sherman [3], the energy equation, which describes the heat transport and is to be solved here, is given by

$$\rho \frac{Dh}{Dt} - \frac{Dp}{Dt} = \mathrm{div}(\lambda \,\mathrm{grad}\, T) + \Phi + \vec{E}^{+} \cdot \vec{j}^{+}, \tag{1}$$

where the substantial quantities are

$$\vec{E}^{+} = \vec{E} + \vec{v} \times \vec{B}, \tag{2}$$

$$\vec{j}^{+} = \vec{j}_c = \vec{j} - \rho_e \cdot \vec{v} \tag{3}$$

and the dissipation function is

$$\Phi = \sum_i \sum_j \tau_{ij}(\partial v_j/\partial x_i). \tag{4}$$

For the components of the shear stress tensor one can write

$$\tau_{ij} = \eta(\partial v_i/\partial x_j + \partial v_j/\partial x_i) - (2/3)\eta\,\delta_{ij}\,\mathrm{div}\,\vec{v}. \tag{5}$$

The generalized Ohm's law for weakly ionized fluids expresses the current density in terms of electromagnetic fields. It is derived by Sutton and Sherman [3] as

$$\vec{j}_c = \sigma \vec{E}^{+} - (\beta_e/B)(\vec{j}_c \times \vec{B}) + f^2 \beta_e \beta_I [(\vec{B}/B)(\vec{B}\vec{j}_c/B) - \vec{j}_c]. \tag{6}$$

This version of Ohm's law considers the anisotropy of electrical conductivity. The first term on the right side of Eq.(6) gives the influence of electric field. The second term considers the Hall effect. The last term introduces ion slip. The ion slip term is obviously important for slightly ionized gases for which the mass fraction of unionized particles, f, is nearly equal to unity, when the magnetic field is large.

It is clear that it will be extremely difficult to solve the energy Eq.(1) in its general form. Consequently, some simplifications must be introduced, if one is to proceed at all.

### 2.2. Simplified Equations

The MHD channel under study is shown in Fig.1. To determine the temperature field from Eq.(1), the following limitations are introduced.

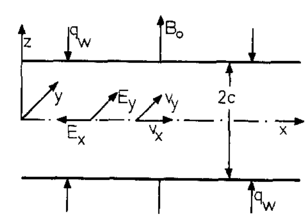


Fig.1. MHD channel under investigation

Geometrical Assumptions

G1. The channel is of constant cross section.

G2. The channel length in x direction and the channel breadth in y direction are much greater than the channel height in z direction.

G3. The electrodes in y direction are segmented infinitely finely in order to allow an axial electric field to develop so that no net axial current will flow.

Fluid Dynamic Assumptions

F1. The laminar flow and the temperature field are steady and fully developed.

F2. The fluid properties are constant.

F3. The Lorentz force is the only external force influencing the fluid motion.

F4. The pressure work is not considered in the energy equation.

Electromagnetic Assumptions

E1. The channel walls in z direction are ideal insulators.

E2. The scalar electrical conductivity is constant.

E3. The flow is free from charge density.

E4. The applied magnetic field is uniform and is much greater then the induced magnetic field; $Re_{mag} \ll 1$.

To summarize, we have

$$\vec{B} = B_x, B_y, B_z; B_x, B_y \ll B_z = B_0 = \text{const.}; \tag{7a}$$

$$\vec{j} = j_x, j_y, 0; \tag{7b}$$

$$\vec{v} = v_x, v_y, 0; \tag{7c}$$

$$\vec{E} = E_x = \text{const.}, E_y = \text{const.}, E_z. \tag{7d}$$

Using Eq. (7), the generalized Ohm's law (6) may be expanded into its components as

$$j_x = \sigma'[(E_x + v_y B_0) - \beta'(E_y - v_x B_0)]/\beta_4, \tag{8a}$$

$$j_y = \sigma'[(E_y - v_x B_0) + \beta'(E_x + v_y B_0)]/\beta_4, \tag{8b}$$

where

$$\beta_1 = f^2 \beta_e (B_0/B) \beta_I (B_0/B), \tag{9a}$$

$$\beta_2 = \beta_e (B_0/B), \ \beta_3 = \sqrt{1 + \beta'^2}, \ \beta_4 = 1 + \beta'^2, \tag{9b}$$

$$\beta' = \beta_2/(1 + \beta_1), \ \sigma' = \sigma/(1 + \beta_1). \tag{9c}$$

It is seen that the presense of ion slip reduces the electrical conductivity $\sigma$ and Hall parameter $\beta_2$ by a factor $(1 + \beta_1)$. For easy treatment of governing equations, the following dimensionless quantities are introduced:

$$\bar{x} = x/c, \ \bar{y} = y/c, \ \bar{z} = z/c, \ p_0 = p(\bar{x} = 0), T_0 = T(\bar{x} = 0, \bar{z}),$$

$$\bar{v}_x = v_x/v_{x,m}, \ \bar{v}_y = v_y/v_{x,m}, \ v_{x,m} = (1/A) \cdot \int_A v_x dA,$$

$$T_{ref} = cq_w/\lambda, \ \bar{T} = (T - T_0)/T_{ref}, \ \bar{p} = (p - p_0)/(\rho v_{x,m}^2), \tag{10a}$$

$$\bar{j}_x = j_x/(\sigma' v_{x,m} B_0), \ \bar{j}_y = j_y/(\sigma' v_{x,m} B_0),$$

$$\bar{E}_x = E_x/(v_{x,m} B_0), \ \bar{E}_y = E_y/(v_{x,m} B_0),$$

$$Re = v_{x,m} c/\nu, \ Pr = \nu \rho c_p/\lambda, \ Pe = RePr,$$

$$Ec = v_{x,m}^2/(c_p T_{ref}), \ Br = EcPr, \tag{10b}$$

$$Ha = cB_0 \sqrt{\sigma/\eta}, \ Ha' = cB_0 \sqrt{\sigma'/\eta}, \ Re_{mag} = cv_{x,m} \sigma' \mu.$$

Considering these dimensionless quantities and respecting the restrictions mentioned, the simplified energy Equation can be derived from the generalized energy Eq. (1) as

$$Pe \bar{v}_x (\partial \bar{T}/\partial \bar{x}) = (\partial^2 \bar{T}/\partial \bar{z}^2) + EcPr[\bar{Q}_v + (Ha')^2 \bar{Q}_j]. \tag{11}$$

The functions, which express the internal heat generation due to viscous dissipation and Joule heating, are given by (for constants see appendix)

$$\bar{Q}_v = (d\bar{v}_x/d\bar{z})^2 + (d\bar{v}_y/d\bar{z})^2$$
$$= (1/2)(Ha_6/B_s)[\cosh(2Ha_r \bar{z}) - \cos(2Ha_i \bar{z})], \tag{12a}$$

$$\bar{Q}_j = \bar{j}_x(\bar{E}_x + \bar{v}_y) + \bar{j}_y(\bar{E}_y - \bar{v}_x) = (\bar{j}_x)^2 + (\bar{j}_y)^2$$
$$= (1/\beta_4)[(\bar{E}_x + \bar{v}_y)^2 + (\bar{E}_y - \bar{v}_x)^2]. \tag{12b}$$

Employing the Eqs. (8) and (10), the dimensionless current densities can be written as

$$\bar{j}_x = (1/\beta_4)[(\bar{E}_x + \bar{v}_y) - \beta'(\bar{E}_y - \bar{v}_x)], \tag{13a}$$

$$\bar{j}_y = (1/\beta_4)[(\bar{E}_x + \bar{v}_y)\beta' + (\bar{E}_y - \bar{v}_x)]. \tag{13b}$$

The solution of Eq. (11) is the nucleus of the present paper and is derived in the following section.

### 2.3. Solution of the Energy Equation

The analysis is simplified by the fact that the energy Eq. (11) is a linear partial differential equation. Hence, the solution can be found as three smaller parts, which are combined to build the complete temperature field. By superposition the total solution is given by

$$\bar{T}(\bar{x},\bar{z}) = \bar{T}_q(\bar{x},\bar{z}) + \bar{T}_v(\bar{x},\bar{z}) + \bar{T}_j(\bar{x},\bar{z}). \tag{14}$$

In Eq. (14), $\bar{T}_q$ defines the temperature distribution, which takes into account the specified uniform heat flux $q_w$ at the channel walls but does not consider any kind of internal heat generation within the fluid. $\bar{T}_v$ describes the temperature distribution, which is caused by the viscous dissipation only. $\bar{T}_j$ expresses the temperature distribution, which is created by the Joule heating only. Both $\bar{T}_v$ and $\bar{T}_j$ do not consider the heat transfer at channel walls. The separation of the total temperature field (14) into smaller parts does not only simplify the analysis but also allows to estimate the contribution of each part. From Eqs. (11) and (14), three partial differential equations can be obtained:

$$Pe\bar{v}_x(\partial\bar{T}_q/\partial\bar{x}) = (\partial^2\bar{T}_q/\partial\bar{z}^2), \tag{15a}$$

$$Pe\bar{v}_x(\partial\bar{T}_v/\partial\bar{x}) = (\partial^2\bar{T}_v/\partial\bar{z}^2) + EcPr\bar{Q}_v, \tag{15b}$$

$$Pe\bar{v}_x(\partial\bar{T}_j/\partial\bar{x}) = (\partial^2\bar{T}_j/\partial\bar{z}^2) + EcPr(Ha')^2\bar{Q}_j. \tag{15c}$$

To solve the Eq. (15), the following conditions are applied:

Condition for constant wall heat flux:

$$|\bar{z}| = 1 : (\partial\bar{T}_q/\partial\bar{z}) = 1. \tag{16a}$$

Condition for zero heat transfer at channels walls:

$$|\bar{z}| = 1 : (\partial\bar{T}_v/\partial\bar{z}) = (\partial\bar{T}_j/\partial\bar{z}) = 0. \tag{16b}$$

Symmetry condition:

$$\bar{z} = 0 : (\partial\bar{T}_q/\partial\bar{z}) = (\partial\bar{T}_v/\partial\bar{z}) = (\partial\bar{T}_j/\partial\bar{z}) = 0. \tag{16c}$$

Condition for fully developed temperature distribution:

$$(\partial\bar{T}_q/\partial\bar{x}) = \text{const.},\ (\partial\bar{T}_v/\partial\bar{x}) = \text{const.},\ (\partial\bar{T}_j/\partial\bar{x}) = \text{const.}. \tag{16d}$$

Condition for an overall energy balance:

$$Pe\frac{\partial}{\partial\bar{x}}\int_0^1 \bar{v}_x\bar{T}_q d\bar{z} = 1, \tag{16e}$$

$$Pe\frac{\partial}{\partial\bar{x}}\int_0^1 \bar{v}_x\bar{T}_v d\bar{z} = EcPr\int_0^1 \bar{Q}_v d\bar{z}, \tag{16f}$$

$$Pe\frac{\partial}{\partial\bar{x}}\int_0^1 \bar{v}_x\bar{T}_j d\bar{z} = EcPr(Ha')^2\int_0^1 \bar{Q}_j d\bar{z}. \tag{16g}$$

The velocity field, which is to be inserted into the Eq. (15), was derived by Javeri [4] from the Navier Stokes equation of motion as (for various constants see appendix)

$$\bar{v}_x = (W_1Z_i - W_2Z_r + W_3)/B_s, \tag{17a}$$

$$\bar{v}_y = (-V_1Z_i - V_2Z_r + V_3)/B_s, \tag{17b}$$

where

$$Z_r = \cosh(Ha_r\bar{z})\cos(Ha_i\bar{z}), \tag{17c}$$

$$Z_i = \sinh(Ha_r\bar{z})\sin(Ha_i\bar{z}). \tag{17d}$$

This velocity field satisfies the conditions:

$$|\bar{z}| = 1 : \bar{v}_x = \bar{v}_y = 0, \tag{18a}$$

$$\bar{z} = 0 : (\partial\bar{v}_x/\partial\bar{z}) = (\partial\bar{v}_y/\partial\bar{z}) = 0, \tag{18b}$$

$$\bar{v}_{x,m} = \int_0^1 \bar{v}_x d\bar{z} = 1,\quad \bar{v}_{y,m} = \int_0^1 \bar{v}_y d\bar{z} = 0. \tag{18c}$$

Before proceeding further, an expression for the axial electric field is needed. It is determined by requiring the condition for no net axial current flow, i.e.

$$\int_0^1 \bar{J}_x d\bar{z} = 0. \tag{19a}$$

From Eqs. (13) and (18), the result is readily found to be

$$\bar{E}_x = \beta'(\bar{E}_y - 1). \tag{19b}$$

To determine the axial temperature gradients, the energy Eq. (15) is integrated over the channel cross section (for different constants see appendix):

$$K_q = Pe(\partial\bar{T}_q/\partial\bar{x}) = 1, \tag{20a}$$

$$K_v = Pe(\partial\bar{T}_v/\partial\bar{x})/(EcPr) = \bar{Q}_{v,m} = \int_0^1 \bar{Q}_v d\bar{z}$$
$$= (Ha_6/B_s)(1/4)(S_{hr2}/Ha_r - S_{ii2}/Ha_i), \tag{20b}$$

$$K_j = Pe(\partial\bar{T}_j/\partial\bar{x})/(EcPr) = (Ha')^2\bar{Q}_{j,m} = (Ha')^2\int_0^1 \bar{Q}_j d\bar{z}$$
$$= H_{20}\Big\{E_3 - 2\bar{E}_y + (Ha_3/B_s)\Big[(1/4)(S_{hr2}/Ha_r + S_{ii2}/Ha_i) -$$
$$-(2/Ha_3)(C_r D_1 + C_i D_2) + C_{r1}\Big]\Big\}. \tag{20c}$$

Respecting the conditions (16), one can deduce from the energy Eq. (15), after an extensive calculation, the temperature distribution as follows (for constants see appendix):

$$\bar{T}_q = \bar{x}/Pe + F_q, \tag{21a}$$

$$\bar{T}_v/(EcPr) = K_v(\bar{x}/Pe + F_q) -$$
$$- [Ha_6(Z_{13}/H_{13} + Z_{14}/H_{14})/(8B_s) - C_2], \tag{21b}$$

$$\bar{T}_j/(EcPr) = K_j\bar{x}/Pe + (K_j + 2\bar{E}_y H_{20})F_q - H_{20}\Big\{E_3\bar{z}^2/2 +$$
$$+ (2\bar{E}_x/B_s)\Big[V_3\bar{z}^2/2 - (S_1 Z_i + S_2 Z_r)/Ha_6\Big] +$$
$$+ (Ha_3/B_s)\Big[(1/8)(Z_{13}/H_{13} - Z_{14}/H_{14}) -$$
$$-(2/Ha_6)(S_3 Z_i + S_4 Z_r) + C_{r1}\bar{z}^2/2\Big] - C_3\Big\}, \tag{21c}$$

where

$$Z_{13} = \cosh(2Ha_r\bar{z}), \quad Z_{14} = \cos(2Ha_i\bar{z}), \tag{21d}$$

$$F_q = \left(F_2\bar{z}^2 - F_3 Z_i - F_4 Z_r\right)/F_1 - F_5. \tag{21e}$$

Defining the fluid mean temperature as

$$\bar{T}_m = \frac{\int_0^1 \bar{T}\bar{v}_x d\bar{z}}{\bar{v}_{x,m}}, \tag{22}$$

one can derive from Eq. (21), the following expressions for the mean temperature

$$\bar{T}_m = [1 + EcPr(K_v + K_j)](\bar{x}/Pe), \tag{23a}$$

$$\bar{T}_{q,m} = \bar{x}/Pe, \quad \bar{T}_{v,m}/(EcPr) = K_v(\bar{x}/Pe), \tag{23b}$$

$$\bar{T}_{j,m}/(EcPr) = K_j(\bar{x}/Pe). \tag{23c}$$

The Nusselt number, which describes the heat transfer at channel walls, is given by

$$Nu = cq_w/[\lambda(T_w - T_m)] = c\,|\partial T/\partial z|_w/(T_w - T_m)$$
$$= 1/(\bar{T}_w - \bar{T}_m), \tag{24a}$$

where

$$(\bar{T}_w - \bar{T}_m) = (\bar{T}_w - \bar{T}_m)_q + (\bar{T}_w - \bar{T}_m)_v + (\bar{T}_w - \bar{T}_m)_j. \tag{24b}$$

All the three terms on the right side of Eq. (24b) can be determined from the Eqs. (21) and (23). Since the closed form solution of temperature field (21) is very complicated, it is advisable to check its correctness. Therefore, the energy Eq. (15) was integrated numerically as follows:

$$\bar{T}_q = \bar{x}/Pe + F_{q1} - \int_0^1 F_{q1}\bar{v}_x d\bar{z}, \tag{25a}$$

$$\bar{T}_v/(EcPr) = K_v(\bar{x}/Pe) + F_{v1} - \int_0^1 F_{v1}\bar{v}_x d\bar{z}, \tag{25b}$$

$$\bar{T}_j/(EcPr) = K_j(\bar{x}/Pe) + F_{j1} - \int_0^1 F_{j1}\bar{v}_x d\bar{z}, \tag{25c}$$

where

$$F_{q1} = \int_0^{\bar{z}} (\bar{z} - \bar{z}')\bar{v}_x(\bar{z}')d\bar{z}', \tag{25d}$$

$$F_{v1} = \int_0^{\bar{z}} (\bar{z} - \bar{z}')[K_v\bar{v}_x(\bar{z}') - \bar{Q}_v(\bar{z}')]d\bar{z}', \tag{25e}$$

$$F_{j1} = \int_0^{\bar{z}} (\bar{z} - \bar{z}')\Big[K_j\bar{v}_x(\bar{z}') - (Ha')^2\bar{Q}_j(\bar{z}')\Big]d\bar{z}', \tag{25f}$$

$\bar{z}'$ : Integration variable.

The comparison between the temperature field (21) and that according to Eq. (25), which were evaluated for a sample set of parameters: $Ha' = 6$, $\beta' = 2$ and $\bar{E}_y = 1/2$, indicated an excellent agreement.

## 3. Result

In section 2.3, the temperature field is determined as a function of $\bar{x}/Pe$ and $\bar{z}$ as well as of parameters $Ha'$, $\beta'$, $\bar{E}_y$, and EcPr.

In Table 1, the functions, which describe the fluid motion and the heat transfer, are given for two limiting cases $\beta' \to 0$ and $\beta' \to \infty$ keeping Ha' = const. The axial velocity profile changes from Hartmann type at $\beta' \to 0$ to a Poiseuille type at $\beta' \to \infty$.

Table 1. Hydrodynamic fields and current densities at $\beta' \to 0$ and $\beta' \to \infty$ for Ha' = const.

| Function | $\beta' \to 0$ | $\beta' \to \infty$ |
|---|---|---|
| $\bar{v}_x$ | $h_1(c_1-g_1)$ | $(3/2)(1-\bar{z}^2)$ |
| $-Re(\partial\bar{p}/\partial\bar{x})$ | $h_3[Ha'/(Ha'-s_1/c_1)-\bar{E}_y]$ | $3+h_3(1-\bar{E}_y)$ |
| $\bar{v}_y$, $\bar{j}_x$ $-Re(\partial\bar{p}/\partial\bar{y})$ | 0 | 0 |
| $\bar{j}_y$ | $(\bar{E}_y-\bar{v}_x)$ | $(\bar{E}_y-1)$ |
| $\bar{Q}_v$ | $[h_3\sinh(Ha'\bar{z})/h_o]^2$ | $9\bar{z}^2$ |
| $\bar{Q}_j$ | $(\bar{E}_y-\bar{v}_x)^2$ | $(\bar{E}_y-1)^2$ |
| $\bar{T}_q-\bar{x}/Pe$ | $f_1 - d_1$ | $(6\bar{z}^2-\bar{z}^4-39/35)/8$ |
| $\bar{T}_v/(EcPr)$ | $a_2[\bar{x}/Pe+(f_1-d_1)]-(f_2-d_2)$ | $3\bar{x}/Pe + 9f_4/8$ |
| $\bar{T}_j/(EcPr)$ | $b_3\bar{x}/Pe + (b_3+2\bar{E}_y h_3)(f_1-d_1) - h_3(f_3-d_3)$ | $[Ha'(\bar{E}_y-1)]^2 \cdot [\bar{x}/Pe + f_4/8]$ |

$c_1 = \cosh(Ha')$; $c_2 = (c_1)^2$; $s_1 = \sinh(Ha')$; $s_2 = \sinh(2Ha')$;
$s_3 = \sinh(3Ha')$; $e_2 = (\bar{E}_y)^2$; $h_o = Ha'c_1-s_1$; $h_1 = Ha'/h_o$;
$h_2 = (h_1)^2$; $h_3 = (Ha')^2$; $h_4 = Ha'h_3$; $h_5 = 2Ha'$;
$r_1 = c_1(2/3+4/h_3)-2(2+h_3)s_1/h_4$; $r_2 = s_2/h_5-1$;
$r_3 = (c_1s_2-s_3/3-s_1)/Ha'$; $d_1 = h_2(c_1r_1/2-r_2/h_3)/2$;
$d_2 = h_1h_2h_3[r_3/(8h_3)-r_1/4]/2$;
$d_3 = h_1\{e_2r_1/2+h_2[r_1(1+2c_2)/4-2c_1r_2/h_3+r_3/(8h_3)]\}/2$;
$a_2 = h_2h_3r_2/2$; $b_3 = h_3[2e_2-4\bar{E}_y+h_2(1+2c_2-3s_2/h_5)]/2$;
$g_1 = \cosh(Ha'\bar{z})$; $g_2 = \cosh(2Ha'\bar{z})$; $f_1 = h_1(c_1\bar{z}^2/2-g_1/h_3)$;
$f_2 = h_2h_3[g_2/(8h_3)-\bar{z}^2/4]$; $f_4 = 2\bar{z}^2 - \bar{z}^4 - 11/35$;
$f_3 = e_2\bar{z}^2/2 + h_2[\bar{z}^2(1+2c_2)/4 - 2c_1g_1/h_3 + g_2/(8h_3)]$.

Since the influence of Ha' and $\beta'$ on the temperature distribution $\bar{T}_q$ is already discussed by Javeri [4], the attention is paid mainly to the viscous dissipation and Joule heating. To assess the influence of Ha' and $\beta'$ on the viscous dissipation, which does not depend upon $\bar{E}_y$, the distribution of viscous dissipation and the temperature profile caused by it are presented in Fig.2 for an arbitrarily selected value of Ha' = 6. The axial temperature gradient and the difference between the wall and mean temperature due to the viscous dissipation are given in Fig.3 as well as in Table 2 as a function of Ha' and $\beta'$. Since the transverse gradient of the axial velocity, which determines the viscous dissipation significantly, is in the vicinity of the channel walls far greater than that in the middle of the channel, the major part of the viscous dissipation is confined in the magnetic boundary layer near

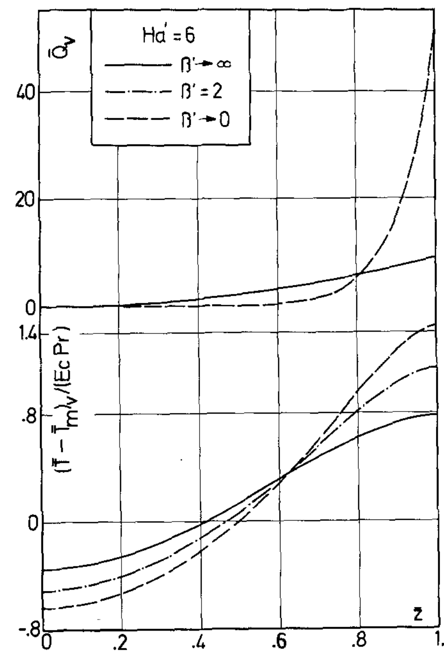


Fig.2. Viscous dissipation and temperature profile caused by it for Ha' = 6; Eqs.(12) and (21)

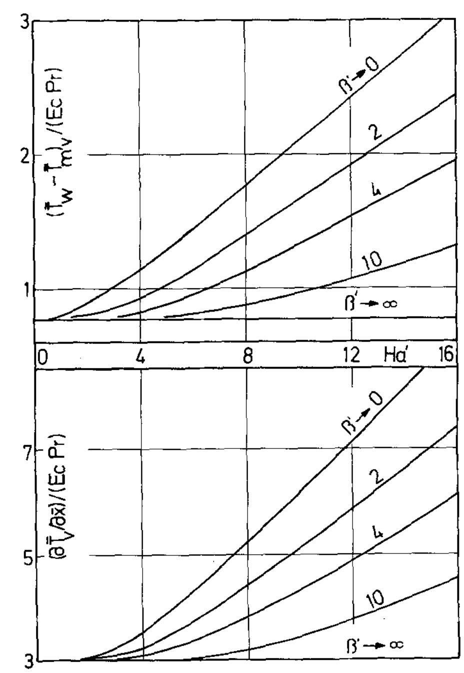


Fig.3. $(\partial\bar{T}_v/\partial\bar{x})/(EcPr)$ and $(\bar{T}_w-\bar{T}_m)_v/(EcPr)$ = fct(Ha', $\beta'$); Eqs. (20) and (21)

the channel walls. This means an augmentation of the heat flux near the walls. From Figs. 2 and 3 as well as from Table 2 one can conclude:

| | $\bar{v}_x$ profile tends to | $\frac{(\partial \bar{T}_v/\partial \bar{x})}{EcPr}$ | $\frac{(\bar{T}_w - \bar{T}_m)_v}{EcPr}$ |
|---|---|---|---|
| Ha' = const. β' increases | Poiseuille type | decreases | decreases |
| Ha' increases β' = const. | Hartmann type | increases | increases |

Table 2. Axial temperature gradient and difference between the wall and mean temperature due to viscous dissipation

| Ha' | β' = 0 | 2 | 4 | 10 | 20 | ∞ |
|---|---|---|---|---|---|---|
| | | | $(\partial \bar{T}_v/\partial \bar{x})/(EcPr)$ | | | |
| 2 | 3.06633 | 3.01697 | 3.00526 | 3.00090 | 3.00023 | 3 |
| 4 | 3.53252 | 3.21187 | 3.07720 | 3.01421 | 3.00363 | |
| 6 | 4.31929 | 3.71013 | 3.32521 | 3.06926 | 3.01820 | |
| 10 | 6.17284 | 5.11824 | 4.32812 | 3.43866 | 3.13259 | |
| 16 | 9.10222 | 7.40140 | 6.12533 | 4.55811 | 3.67331 | |
| | | | $(\bar{T}_w-\bar{T}_m)_v/(EcPr)$ | | | |
| 2 | .879928 | .799616 | .780194 | .772934 | .771809 | .771429 |
| 4 | 1.14049 | .922494 | .827392 | .781814 | .774086 | |
| 6 | 1.45194 | 1.14458 | .947376 | .809847 | .781578 | |
| 10 | 2.10397 | 1.65927 | 1.33876 | .969720 | .832975 | |
| 16 | 3.09623 | 2.43658 | 1.95724 | 1.38425 | 1.05114 | |

In general, the effect of β' on the shape of the axial velocity profile and on the viscous dissipation can be noticed clearly, as Ha' increases. The results indicate that the significant error may be introduced in the prediction of the quantities, which express the heat transport, for large Ha', if β' is neglected in the analysis, for instance,

$$\frac{(\partial \bar{T}_v/\partial \bar{x})(Ha' = 10,\ \beta' \to 0)}{(\partial \bar{T}_v/\partial \bar{x})(Ha' = 10,\ \beta' \to \infty)} = 2.06,$$

$$\frac{(\bar{T}_w - \bar{T}_m)_v(Ha' = 10,\ \beta' \to 0)}{(\bar{T}_w - \bar{T}_m)_v(Ha' = 10,\ \beta' \to \infty)} = 2.72.$$

It is more difficult to assess the temperature distribution due to the Joule heating because it is a function of Ha', β' and $\bar{E}_y$. To save place here, the attention is dedicated to two special cases of $\bar{E}_y$. They are $\bar{E}_y = 0$ (short circuit) and $\bar{E}_y = 1$ (open circuit). To understand the effect of Ha' and β' on the Joule heating, the distribution of Joule heating and the temperature profile originated by it are illustrated in Fig. 4 for an arbitrarily selected

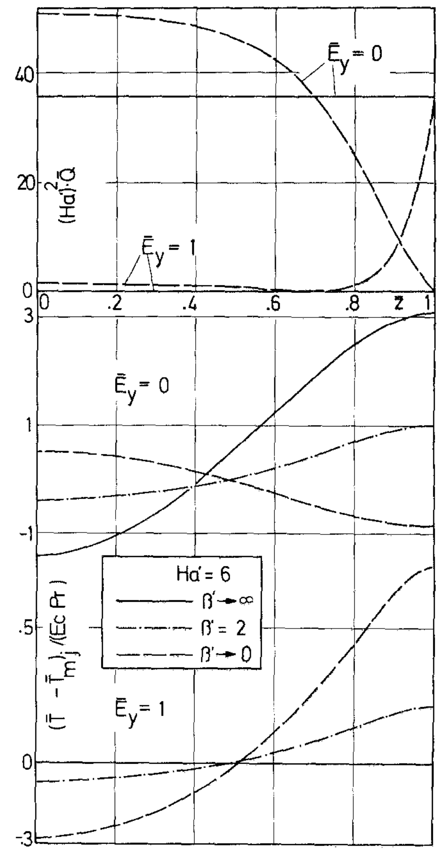


Fig. 4. Joule heating and temperature profile caused by it for Ha' = 6; Eqs. (12) and (21)

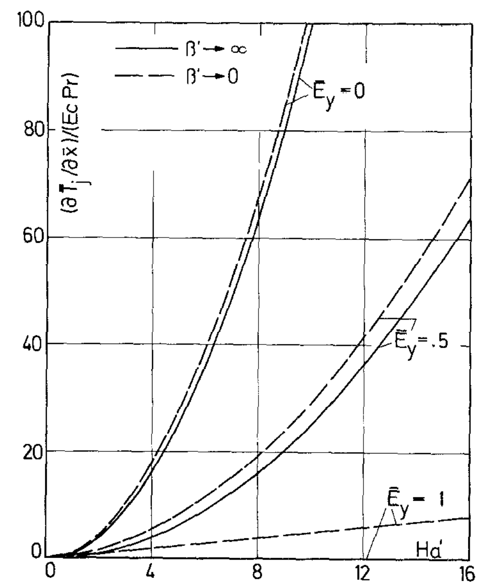


Fig. 5. $(\partial \bar{T}_j/\partial \bar{x})/(EcPr) = fct(Ha', \beta', \bar{E}_y)$; Eq. (20)

value of Ha' = 6 and for $\bar{E}_y = 0$ and $\bar{E}_y = 1$. In case of short circuit situation and $\beta' = 0$, the Joule heating is almost equally distributed all over the channel; for $\beta' \to \infty$ it tends to a constant value. In case of open circuit condition and $\beta' = 0$, the major part of the Joule heating is confined in the vicinity of the channel walls. Thus it acts as a wall heat flux; for $\beta' \to \infty$ it tends to zero. In Fig.5 and in Table 3, the axial temperature gradient due to Joule heating according to Eq.(20) is given. For short

Table 3. Axial temperature gradient and difference between the wall and mean temperature due to Joule heating

| Ha' | ß' = 0 | 2 | 4 | 10 | 20 | ∞ | $\bar{E}_y$ |
|---|---|---|---|---|---|---|---|
| | | | $(\partial T_j/\partial \bar{x})/(EcPr)$ | | | | |
| 2 | 4.65588 | 4.15261 | 4.04639 | 4.00790 | 4.00199 | 4 | |
| 4 | 17.7960 | 16.5260 | 16.1760 | 16.0313 | 16.0080 | 16 | |
| 6 | 38.8806 | 36.9469 | 36.3556 | 36.0688 | 36.0178 | 36 | 0 |
| 10 | 104.938 | 101.707 | 100.714 | 100.171 | 100.048 | 100 | |
| 16 | 263.964 | 258.784 | 257.188 | 256.321 | 256.106 | 256 | |
| 2 | 1.65588 | 1.15261 | 1.04639 | 1.00790 | 1.00199 | 1 | |
| 4 | 5.79605 | 4.52604 | 4.17596 | 4.03130 | 4.00796 | 4 | |
| 6 | 11.8806 | 9.94692 | 9.35555 | 9.06882 | 9.01779 | 9 | .5 |
| 10 | 29.9383 | 26.7067 | 25.7136 | 25.1706 | 25.0478 | 25 | |
| 16 | 71.9644 | 66.7837 | 65.1884 | 64.3209 | 64.1059 | 64 | |
| 2 | .655884 | .152612 | .046385 | .007901 | .001994 | 0 | |
| 4 | 1.79605 | .526035 | .175955 | .031302 | .007956 | 0 | |
| 6 | 2.88061 | .946917 | .355549 | .068824 | .017792 | 0 | 1 |
| 10 | 4.93827 | 1.70674 | .713567 | .170550 | .047755 | 0 | |
| 16 | 7.96444 | 2.78371 | 1.18839 | .320874 | .105926 | 0 | |
| | | | $(\bar{T}_w-\bar{T}_m)_j/(EcPr)$ | | | | |
| 2 | -.161910 | .218035 | .304412 | .336277 | .341195 | .342857 | |
| 4 | -.496462 | .672564 | 1.11809 | 1.32481 | 1.35951 | 1.37143 | |
| 6 | -.851906 | 1.05104 | 2.13868 | 2.88024 | 3.03150 | 3.08571 | 0 |
| 10 | -1.54385 | 1.54743 | 3.79356 | 6.82404 | 8.02546 | 8.57143 | |
| 16 | -2.55895 | 2.19337 | 5.70505 | 11.7693 | 16.9911 | 21.9429 | |
| 2 | -.086714 | .041515 | .072007 | .083362 | .085120 | .085714 | |
| 4 | -.265854 | .097148 | .252216 | .326069 | .338563 | .342857 | |
| 6 | -.451922 | .088932 | .447314 | .700564 | .752709 | .771429 | .5 |
| 10 | -.805162 | -.00840 | .668823 | 1.60352 | 1.97436 | 2.14286 | |
| 16 | -1.31635 | -.15989 | .860137 | 2.62652 | 4.10107 | 5.48571 | |
| 2 | .138876 | .030906 | .009312 | .001581 | .000399 | 0 | |
| 4 | .425972 | .110708 | .035748 | .006277 | .001592 | 0 | |
| 6 | .748030 | .212317 | .073997 | .013856 | .003564 | 0 | 1 |
| 10 | 1.41089 | .434699 | .163002 | .035040 | .009609 | 0 | |
| 16 | 2.41142 | .782941 | .308663 | .071904 | .021862 | 0 | |

circuit situation, this quantity is nearly independant of of $\beta'$, e.g.

$$\frac{(\partial \bar{T}_j/\partial \bar{x})(\bar{E}_y = 0,\ Ha' = 10,\ \beta' \to 0)}{(\partial \bar{T}_j/\partial \bar{x})(\bar{E}_y = 0,\ Ha' = 10,\ \beta' \to \infty)} = 1.05.$$

In case of open circuit condition, the axial temperature gradient $(\partial \bar{T}_j/\partial \bar{x})$ depends upon $\beta'$ distinclty. In Fig.6 as well as in Table 3, the difference between the wall and mean temperature due to Joule heating according to Eq.(21) is presented. With the help of Fig.4, one can understand the curves of Fig.6. For Ha' = const. and short circuit condition, the Joule heating near the wall increases as $\beta'$ increases. For open circuit situation and Ha' = const., the Joule heating near the wall decreases as $\beta'$ increases.

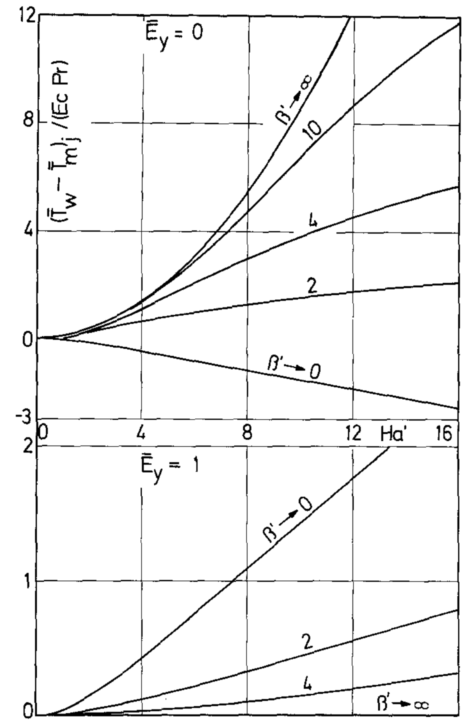


Fig.6. $(\bar{T}_w - \bar{T}_m)_j/(EcPr) = fct(Ha', \beta', \bar{E}_y)$; Eq.(21)

The solution derived and the results presented in this paper can be employed to decide which of the two arts of the internal heat generation is important and to estimate $\beta'$, beyond which one can practically set $\beta'$ equal to infinity, for a given combination of parameters Ha' and $\bar{E}_y$.

To calculate the Nusselt number according to Eq.(24), one must also know the value of the dimensionless group EcPr. The complete presentation of the Nusselt number for the different values of the parameters Ha', $\beta'$, $\bar{E}_y$ and EcPr would enlarge this paper significantly. Accordingly, to obtain a general survey of the combined influence of these four parameters on the heat transfer at the channel walls, the Nusselt number is illustrated in Fig.7 for the extreme values of $\beta'$ and for the special values of $\bar{E}_y$. From Fig.7 one can deduce that a substantial error can be introduced in the prediction of the Nusselt number, depending upon Ha', $\beta'$, $\bar{E}_y$ and EcPr, if the Hall effect is completely neglected. Table 4 shows the Nusselt number for the limiting values of $\beta'$ and for the sample values of Ha', $\bar{E}_y$ and EcPr and gives a general view about the magnitude of the possible maximum error in the determination of Nusselt number, if the Hall

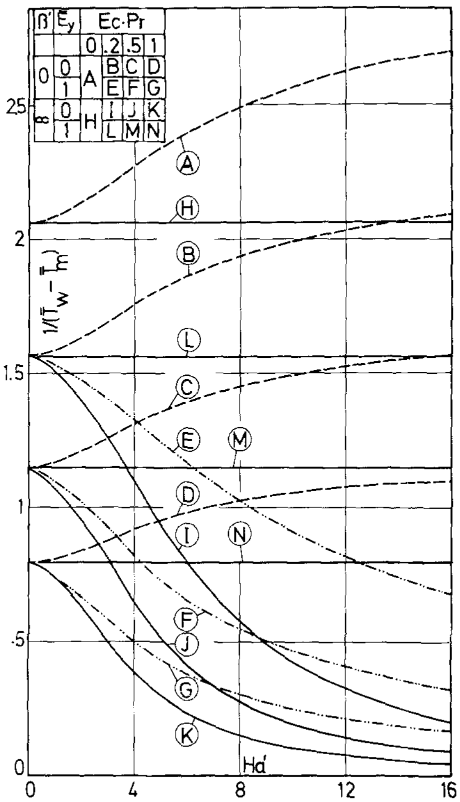


Fig.7. $1/(\overline{T}_w - \overline{T}_m)$ = fct(Ha', β', $\overline{E}_y$, EcPr) ; Eq.(24)

effect is not considered. Form Table 4, one can learn: greater the deviation between the ratio of extreme Nusselt numbers and unity, greater the influence of the reduced Hall parameter β' on the heat transfer at the channel walls. It can be noted that this ratio, depending upon Ha', $\overline{E}_y$ and EcPr, can exceed the range limited by 0.1 and 10.

Finally, it is concluded that the Hall effect and ion slip have significant influence on the limiting, fully developed heat transfer conditions in an MHD channel, and the analysis of the problem by neglecting these effects may result in considerable error in the solutions representing the actual physical conditions.

Table 4. Ratio of Nusselt number at β' → 0 to Nusselt number at β' → ∞

| Ha' | $\overline{E}_y$ | [Nu(β' → 0)]/[Nu(β' → ∞)] | | | |
|---|---|---|---|---|---|
| | | EcPr | | | |
| | | 0 | 0.2 | 0.5 | 1.0 |
| 4 | 0 | 2.27532/2.05882 = 1.105 | 1.75963/1.09375 = 1.609 | 1.31318/.642202 = 2.045 | .922915/.380435 = 2.426 |
| | 1 | | 1.32839/1.56250 = 0.850 | .817844/1.14754 = 0.713 | .498515/.795455 = 0.627 |
| 10 | 0 | 2.56464/2.05882 = 1.246 | 1.99226/.424757 = 4.690 | 1.49258/.193906 = 7.697 | 1.05258/.101744 = 10.35 |
| | 1 | | .915005/1.56250 = 0.586 | .465691/1.14754 = 0.406 | .256097/.795455 = 0.322 |

## 4. Appendix

The constants, which appear in the velocity and temperature fields and depend upon the parameters Ha', β' and $\overline{E}_y$, are listed below.

$\beta_3 = \sqrt{1 + \beta'^2}$; $\beta_4 = 1 + \beta'^2$;

$\beta_r = \sqrt{(1/2)(\beta_3 + 1)}$; $\beta_i = \sqrt{(1/2)(\beta_3 - 1)}$;

$\overline{E}_x = \beta'(\overline{E}_y - 1)$; $E_1 = (\overline{E}_y)^2$; $E_2 = (\overline{E}_x)^2$; $E_3 = E_1 + E_2$;

$Ha_r = Ha'\beta_r/\beta_3$; $Ha_i = Ha'\beta_i/\beta_3$; $H_{13} = (Ha_r)^2$;

$H_{14} = (Ha_i)^2$;

$H_{11} = 9H_{13} + H_{14}$; $H_{12} = H_{13} + 9H_{14}$; $Ha_3 = H_{13} + H_{14}$;

$Ha_4 = H_{13} - H_{14}$;

$Ha_5 = 2Ha_r Ha_i$; $Ha_7 = (Ha_3)^3$; $Ha_6 = (Ha_3)^2$;

$Ha_8 = 2Ha_r$; $Ha_9 = 2Ha_i$; $H_{20} = (Ha')^2/\beta_4$;

$D_r = Ha_r(H_{13} - 3H_{14})$; $D_i = Ha_i(3H_{13} - H_{14})$;

$C_r = \cosh(Ha_r)\cos(Ha_i)$; $C_i = \sinh(Ha_r)\sin(Ha_i)$;

$S_r = \sinh(Ha_r)\cos(Ha_i)$; $S_i = \cosh(Ha_r)\sin(Ha_i)$;

$S_{hr2} = \sinh(Ha_8)$; $S_{ii2} = \sin(Ha_9)$;

$C_{hr2} = \cosh(Ha_8)$; $C_{oi2} = \cos(Ha_9)$;

$S_{r2} = S_{hr2}C_{oi2}$; $S_{i2} = C_{hr2}S_{ii2}$;

$S_{i3} = \cosh(3Ha_r)\sin(Ha_i)$; $S_{r3} = \sinh(3Ha_r)\cos(Ha_i)$;

$S_{r4} = \sinh(Ha_r)\cos(3Ha_i)$; $S_{i4} = \cosh(Ha_r)\sin(3Ha_i)$;

$B_r = Ha_r C_r - Ha_i C_i - S_r$; $B_i = Ha_r C_i + Ha_i C_r - S_i$;

$B_s = (B_r)^2 + (B_i)^2$; $C_{r1} = (C_r)^2 + (C_i)^2$;

$T_r = D_r C_r - D_i C_i$; $T_i = D_r C_i + D_i C_r$;

$W_1 = V_2 = B_r Ha_i - Ha_r B_i$; $W_2 = V_1 = Ha_r B_r + Ha_i B_i$;

$W_3 = W_2 C_r - W_1 C_i$; $V_3 = V_1 C_i + V_2 C_r$;

$S_1 = V_1 Ha_4 + V_2 Ha_5$; $S_2 = V_2 Ha_4 - V_1 Ha_5$;

$S_3 = C_i Ha_4 + C_r Ha_5$; $S_4 = C_r Ha_4 - C_i Ha_5$;

$D_1 = Ha_r S_r + Ha_i S_i$; $D_2 = Ha_r S_i - Ha_i S_r$;

$F_1 = B_s Ha_3$; $F_2 = W_3 Ha_3/2$; $F_3 = Ha_i B_r + Ha_r B_i$;

$F_4 = Ha_r B_r - Ha_i B_i$;

$R_{10} = (Ha_4 C_i - Ha_5 C_r)/Ha_6 - (D_r S_i - D_i S_r)/Ha_7$;

$R_1 = D_2/Ha_3 - 2R_{10}$;

$R_{20} = (Ha_4 C_r + Ha_5 C_i)/Ha_6 - (D_i S_i + D_r S_r)/Ha_7$;

$R_2 = D_1/Ha_3 - 2R_{20}$;

$R_3 = [S_{hr2}/Ha_8 - 1 - (Ha_r S_{r2} + Ha_i S_{i2})/(2Ha_3) + S_{ii2}/Ha_9]/4$;

$R_4 = [(Ha_r S_{r2} + Ha_i S_{i2})/(2Ha_3) + S_{hr2}/Ha_8 + S_{ii2}/Ha_9 + 1]/4$;

$R_5 = (Ha_r S_{i2} - Ha_i S_{r2})/(8Ha_3)$; $R_6 = 1/3$; $R_7 = D_2/Ha_3$;

$R_8 = D_1/Ha_3$;

$F_{51} = F_2 W_1 R_1 - F_2 W_2 R_2 - F_3 W_1 R_3 + F_4 W_2 R_4$;

$F_{52} = (F_3 W_2 - F_4 W_1) R_5 + W_3 (F_2 R_6 - F_3 R_7 - F_4 R_8)$;

$F_5 = (F_{51} + F_{52})/(Ha_3 B_s^2)$;

$G_1 = [(3Ha_r S_{i3} - Ha_i S_{r3})/H_{11} - D_2/Ha_3]/2$;

$G_2 = [(Ha_r S_{i4} - 3Ha_i S_{r4})/H_{12} - D_2/Ha_3]/2$;

$G_3 = [(3Ha_r S_{r3} + Ha_i S_{i3})/H_{11} + D_1/Ha_3]/2$;

$G_4 = [(Ha_r S_{r4} + 3Ha_i S_{i4})/H_{12} + D_1/Ha_3]/2$;

$G_5 = S_{hr2}/Ha_8$;

$G_6 = S_{ii2}/Ha_9$; $G_7 = W_1 R_1 - W_2 R_2 + W_3 R_6$;

$G_8 = W_1 R_3 - W_2 R_5 + W_3 R_7$; $G_9 = W_1 R_5 - W_2 R_4 + W_3 R_8$;

$U_1 = W_1 G_1 - W_2 G_3 + W_3 G_5$; $U_2 = W_1 G_2 - W_2 G_4 + W_3 G_6$;

$C_2 = (1/8)(Ha_6/B_s^2)(U_1/H_{13} + U_2/H_{14})$;

$C_{31} = E_3 G_7/2 + 2\overline{E}_x [V_3 G_7/2 - (S_1 G_8 + S_2 G_9)/Ha_6]/B_s$;

$C_{32} = (U_1/H_{13} - U_2/H_{14})/8 - 2(S_3 G_8 + S_4 G_9)/Ha_6 + C_{r1} G_7/2$;

$C_3 = (C_{31} + Ha_3 C_{32}/B_s)/B_s$.

## References


1. Perlmutter, M.; Siegel, R.: Heat transfer to an electrically conducting fluid flowing in a channel with a transverse magnetic field. NASA TN D-875 (1961)
2. Eraslan, A.H.: Temperature distributions in MHD channels with Hall effect. AIAA J. 7 (1969) 186/188
3. Sutton, G.W.; Sherman, A.: Engineering Magnetohydrodynamics. New York: McGraw-Hill (1965)
4. Javeri, V.: Influence of Hall effect and ion slip on velocity and temperature fields in an MHD channel. Wärme- u. Stoffübertragung 7 (1974) 226/235


Dr.-Ing. V. Javeri
Institut für Kerntechnik der
Technischen Universität Berlin

D-1 Berlin 12
Marchstr. 18
(Deutschland)

Received December 12, 1974